



Thermo-hydraulic design of a horizontal shell and tube heat exchanger for ethanol condensation

Diseño térmico-hidráulico de un intercambiador de calor de tubo y coraza horizontal para la condensación de etanol

Amaury Pérez Sánchez ^{1,*}, Maria Isabel La Rosa Veliz ¹, Zamira María Sarduy Rodríguez ¹, Elizabeth Ranero González ¹, Eddy Javier Pérez Sánchez ²

¹ University of Camagüey “Ignacio Agramonte Loynaz”, Faculty of Applied Sciences, Camagüey, Cuba.

² Company of Automotive Services S.A., Commercial Department, Ciego de Ávila, Cuba.

*amaury.perez84@gmail.com

(recibido/received: 25-abril-2023; aceptado/accepted: 14-agosto-2023)

ABSTRACT

Horizontal shell and tube condensers are widely used in several industrial applications due to its versatility and heat transfer efficacy. In the present work, the thermo-hydraulic design of a horizontal shell and tube heat exchanger intended to condense 25,000 kg/h of a pure ethanol stream was carried out. Several key design parameters were calculated such as the number of tubes, heat transfer area, overall heat transfer coefficient, shell internal diameter, baffle spacing, as well as the pressure drop for both streams. The heat exchanger type is of pull-through floating head, and will present a number of tubes of 731, a heat transfer area of 223.68 m², an overall heat transfer coefficient of 499.36 W/m².°C, a shell internal diameter of 1.684 m and a baffle spacing of 0.674 m. Around 157 kg/s of chilled water will be required for this heat transfer service. The values of both the shell side (10,069.25 Pa) and tube side (42,192.63 Pa) pressure drop are below the maximum values set by the process.

Keywords: Design; Ethanol condensation; Shell and tube heat exchanger; Pressure drop; Heat transfer area.

RESUMEN

Los condensadores de tubo y coraza horizontales son ampliamente usados en varias aplicaciones industriales debido a su versatilidad y eficacia de transferencia de calor. En el presente trabajo, se llevó a cabo el diseño térmico-hidráulico de un intercambiador de calor de tubo y coraza horizontal pretendido para condensar 25 000 kg/h de una corriente de etanol puro. Varios parámetros claves de diseño fueron calculados tales como el número de tubos, área de transferencia de calor, coeficiente global de transferencia de calor, diámetro interno de la coraza, espaciado de los deflectores así como también la caída de presión para ambas corrientes. El tipo de intercambiador de calor será de cabezal flotante y presentará un número de tubos de 731, un área de transferencia de calor de 223,68 m², un coeficiente global de transferencia de calor de 499,36 W/m².°C, un diámetro interno de la coraza de 1,684 m y un espaciado de los deflectores de 0,674 m. Alrededor de 157 kg/s de agua fría serán requeridos para este servicio de transferencia de calor. Los valores de tanto la caída de presión por el lado de la coraza (10

069,25 Pa) como por el lado de los tubos (42 192,63 Pa) están por debajo de los valores máximos fijados por el proceso.

Palabras claves: Diseño; Condensación de etanol; Intercambiador de calor de tubo y coraza; Caída de presión; Área de transferencia de calor.

NOMENCLATURE

a_{ct}	Tube cross sectional area	m^2
a_t	Surface area of one tube	m^2
A_0	Triangular area	m^2
A_s	Cross-flow area between tubes	m^2
C_p	Heat capacity	$\text{kJ/kg}\cdot^\circ\text{C}$
C_t	Clearance required between the outermost tubes in the bundle	m
d_e	Shell-side equivalent diameter	m
d_i	Inside diameter of tube	m
d_o	Outside diameter of tube	m
D_b	Tube bundle diameter	mm
D_s	Shell internal diameter	m
F_t	Temperature correction factor	-
g	Gravitational acceleration	m/s^2
G_s	Shell-side mass velocity	$\text{kg/s}\cdot\text{m}^2$
h	Enthalpy	kJ/kg
$h_{c(a)}$	Mean condensation film coefficient assumed	$\text{W/m}^2\cdot^\circ\text{C}$
$h_{c(c)}$	Mean condensation film coefficient for a tube bundle	$\text{W/m}^2\cdot^\circ\text{C}$
h_t	Tube side heat transfer coefficient	$\text{W/m}^2\cdot^\circ\text{C}$
j_s	Shell-side friction factor	-
j_t	Tube-side friction factor	-
k	Thermal conductivity	$\text{W/m}\cdot^\circ\text{C}$
K_1	Constant	-
l_B	Baffle spacing	m
L_t	Tube length	m
m	Mass flowrate	kg/h
M	Molecular weight	Kg/kmol
n_1	Constant	-
n_t	Number of tube-side passes	-
N_r	Number of tubes in centre row	-
N_{t0}	Number of tubes	-
N_{tr}	Average number of tubes in a vertical tube row	-

p_t	Tube pitch	m
P	Inlet pressure of the vapour stream	bar
P_0	Atmospheric pressure	bar
ΔP_s	Shell side pressure drop	Pa.
ΔP_t	Tube-side pressure drop	Pa
Q	Heat transferred from vapour	kW
R	Fouling factor	$\text{m}^2 \cdot \text{°C}/\text{W}$
R	Parameter	-
Re	Reynolds number	-
S	Parameter	-
t	Temperature of the cold fluid	°C
\bar{t}	Mean temperature of the cold fluid	°C
T	Temperature of the hot fluid	°C
T_c	Condensation temperature of the vapour stream	°C
T_w	Tube wall temperature	°C
\bar{T}	Mean temperature of the hot fluid	°C
\bar{T}_c	Mean temperature of condensate	°C
ΔT_{lm}	Log mean temperature difference	°C
ΔT_m	True temperature difference	°C
U	Overall heat transfer coefficient calculated	$\text{W}/\text{m}^2 \cdot \text{°C}$
U_0	Overall heat transfer coefficient assumed	$\text{W}/\text{m}^2 \cdot \text{°C}$
u	Velocity	m/s
u_s	Shell-side linear velocity	m/s

Greek symbols

ρ	Density	kg/m^3
μ	Viscosity	Pa.s
Γ_h	Condensate loading on a horizontal tube	$\text{kg}/\text{s} \cdot \text{m}$

Subscripts

1	Inlet
2	Outlet
c	Cold fluid
et	Ethanol
L	Liquid
ss	Stainless steel
t	Tube side fluid
v	Vapour
w	Water

1. INTRODUCTION

A heat exchanger is a complex device that provides the transfer of thermal energy between two or more fluids, which are at different temperatures and are in thermal contact with each other. Heat exchangers are used either individually or as components of a large thermal system, in a wide variety of commercial, industrial and household applications, e.g. power generation, refrigeration, ventilating and air-conditioning systems, process, manufacturing, aerospace industries, electronic chip cooling as well as in environmental engineering (Girish *et al.*, 2017). One of the most important heat exchangers used today at industrial scale is the shell and tube heat exchanger (STHE).

The STHE provide a large heat transfer area both economically and practically. The tubes are placed in a bundle and the ends of the tubes are mounted in tube sheets (Figure 1). The tube bundle is enclosed in a cylindrical shell through which the second fluid flows. Most shell-and-tube exchangers used in practice are of welded construction. The shells are built as a piece of pipe with flanged ends and associated/necessary branch connections (Flynn *et al.*, 2019).

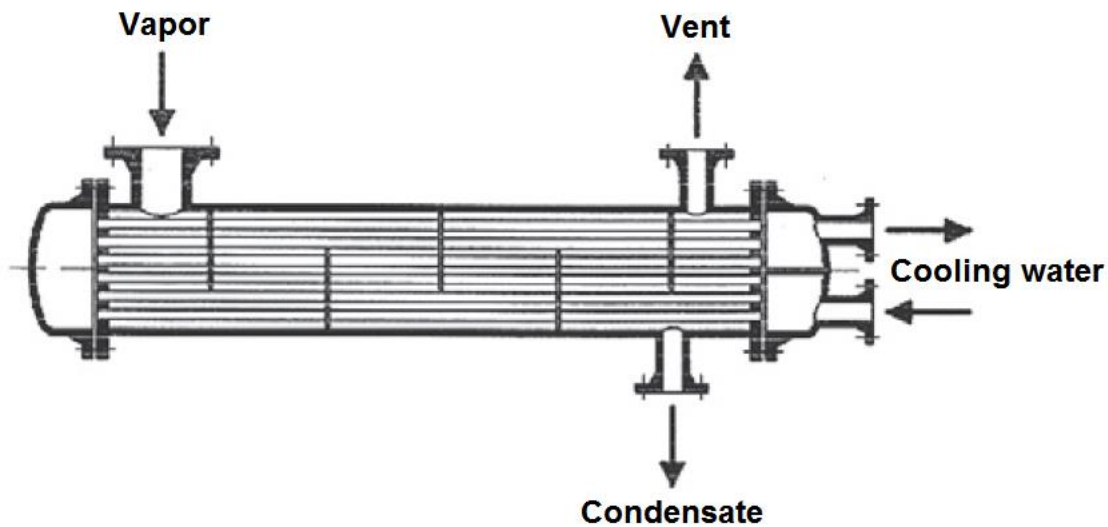


Figure 1. Typical layout of a shell and tube condenser.

Source: Adapated from (Nitsche & Gbadamosi, 2016)

There are vast industrial uses of shell-and-tube heat exchangers. These units are used to heat or cool process fluids, either through a single-phase heat exchanger or a two-phase heat exchanger. In single-phase exchangers, both the tube-side and shell-side fluids remain in the same phase that they enter. In two-phase exchangers (examples include condensers and boilers), the shell-side fluid is usually condensed to a liquid or heated to a gas, while the tube-side fluid usually remains in the same phase. Generally, shell-and-tube exchangers are employed when double pipe exchangers do not provide sufficient area for heat transfer. Thus, when large heat-transfer surfaces are required, they can usually be best obtained by means of shell-and-tube exchangers (Flynn *et al.*, 2019).

According to (Hajabdollahi *et al.*, 2011) they are used to transfer heat between two or more fluids, between a solid surface and a fluid, or between solid particulates and a fluid, at different temperatures and in thermal contact, while there are usually no external heat and work interactions.

The STHE is widely used in many industries, i.e., industrial power plants as condensers, chemical and petrochemical plants as preheating or cooling systems (Chen *et al.*, 2022), as well as refrigeration/air conditioning systems (Hajabdollahi *et al.*, 2011). For example, a condenser is a fundamental equipment in a distillation column system, providing reflux to promote the separation. Condensers may also be found in

certain reaction units, where they are employed to recover a desired product from the outlet stream of a reactor from gaseous components. Condensers are also present in power stations based on Rankine cycle, where they are responsible for the condensation of the turbine exhaust steam. Refrigeration cycles also involve the presence of a condenser, which promotes the heat rejection to the environment. While other kinds of heat exchangers may be employed in some of the aforementioned applications (e.g. gasketed plate, air coolers, etc.), the shell-and-tube heat exchanger is still the main option (Pereira *et al.*, 2021).

Shell and tube condensers are the most commonly used heat exchangers in process industries because of their relatively simple manufacturing and their adaptability to different operating conditions. Although this condenser type distinguishes itself by low-pressure drops with high flow velocities, the capital requirement of it, as well as the associated flow (i.e. the combined power and capital) cost requirement due to pressure drops of the pumped and compressed streams in a unit can be very expensive (Soltan *et al.*, 2004).

Shell-and-tube condensers with condensation on the shell-side are widely used in both process and refrigeration industries. This typically means that, the condensing medium is fed to the top of a shell-and-tube heat exchanger, and then while flowing on the outside of the tubes it condenses, leaving its latent heat to the cooling medium flowing inside the tubes. The condensed liquid is collected at the bottom of the shell where it leaves the condenser. The heat transfer in a shell-and-tube condenser is complicated to predict. Factors such as the complex geometry of the tube bank, effect of the tube surface geometry, vapour shear effects and condensate inundation from the tubes above all have an effect on heat transfer (Karlsson & Vamling, 2005).

Traditionally, there are two approaches that establish the foundation of the design of STHE, which are the so-called Kern (Kern, 1950), and the Bell-Delaware (Bell, 1963) methods (Chen *et al.*, 2022). Traditional design methods of heat exchanger have been developed through optimization of the heat exchanger geometry such as layout, tube pitch, baffle cut, tube diameter, baffle spacing, and so on, while satisfying the heat duty from both the hot and cold fluids (Lim & Choi, 2020).

Since shell and tube type condensers are widely used in refrigeration and heat pump, as well as air-conditioning systems, there has been increasing interest by various researchers on its design and optimization (Hajabdollahi *et al.*, 2011).

Several authors have studied the design of shell and tube condensers. In this sense, (Chen *et al.*, 2022) addressed the issues of STHE design under process uncertainty where the rigorous operating constraints are taken into account to establish the structural design of the STHE while simultaneously incorporating the flexibility index. This study considered the genetic algorithm with rigorous constraints for the STHE design optimization. Also, (Milián *et al.*, 2013) proposed an moving-boundary lumped parameter dynamic model of a shell-and-tube condenser where the mean void fraction (MVF) correlation used can be changed in order to analyze the influence of the MVF correlation on the model performance, comparing the predictions obtained with experimental data using MVF correlations frequently mentioned in the literature. In order to evaluate the performance of the model with each different MVF correlation, a set of experimental tests were performed using R134a as working fluid and varying the main operating variables (refrigerant mass flow rate, secondary fluid mass flow rate and inlet temperature). Likewise, (Feng *et al.*, 2020) studied the constructal design of a shell and tube condenser using ammonia-water as the working fluid, where the linear weighted complex function made up of the entropy generation rate and total pumping power were minimized, while the parameters influencing the optimal results were researched. Similarly, (Hajabdollahi *et al.*, 2011) presented the thermo-economic optimization method of a shell and tube condenser, based on two new optimization approaches, namely genetic and particle swarm algorithms. The procedure used in this work was selected to find the optimal total cost including investment and operation cost of the condenser. Initial cost includes condenser surface area and

operational cost includes pump output power to overcome the pressure loss. Design parameters are tube number, number of tube pass, inlet and outlet tube diameters, tube pitch ratio and tube arrangements. Other authors (Soltan *et al.*, 2004) studied the effect of baffle spacing on heat transfer area and pressure drop for shell side condensation in the most common types of segmentally baffled shell and tube condensers used (TEMA E and J types with conventional tube bundles) Also, as a result of this research, a set of correlation was presented to calculate the optimum baffle spacing. In (Lim & Choi, 2020) a study was carried out consisting in two categories: the first consisted in the integration of an organic Rankine cycle (ORC) with the cold energy of liquid natural gas (LNG) fuelled ships, while the second involved the thermal design of the heat exchanger (condenser) contained in the ORC system. Some parameters such as layout, tube pitch, baffle cut and number of passes were fixed first. Based on various heat transfer coefficients obtained from the literature, the thermal design of the condenser was formulated in order to enable the accurate design of the heat exchangers comprising ORC systems. In another study (Llopis *et al.*, 2008) presented and validated a dynamic mathematical model of a shell-and-tube condenser operating in a vapour compression refrigeration plant. The model was formulated from mass continuity, energy conservation and heat transfer physical fundamentals by using a lumped-parameter formulation for the condenser that is similar to the ones presented by (Deng, 2000), but with some differences in the selection of control volumes and including the refrigerant dynamics in a simplified way. Other authors (Nithyanandam *et al.*, 2021) carried out a study which included the first effort to investigate the techno-economics of enhanced condenser design with nonwetting tube surfaces in a thermoelectric power plant, as well as the quantification of the improvements relative to a baseline condenser design with plain tubes. (Pereira *et al.*, 2021) presented a mathematical programming approach for the determination of the global optimum solutions for the design of horizontal shell-and-tube condensers. The original representation of the design optimization problem corresponds to a mixed-integer nonlinear programming. The application of a set of proper algebraic techniques allowed a mathematical reformulation of the problem, and then represented as an integer linear programming. This new representation of the problem presents two main advantages: it does not depend of initial estimates and always converge to the global optimum solution, thus avoiding drawbacks associated to nonlinear formulations. In (Kapooria *et al.*, 2008) a conceptual technological design aspect of a super vacuum hybrid surface steam condenser was theoretically analyzed. In (Sahajpal & Shah, 2013) the thermal design of a shell and tube desuperheater-condenser for an ammonia-water system was carried out manually using the Kern's method, while the results obtained were compared to obtained by HTRI software. In (Kara, 2014) a computer code based on a simplified model for designing a horizontal shell and tube refrigerant condenser was presented. The model uses three-zone approach for condensing-side and overall approach for the coolant-side of the condenser. Given the thermal and hydraulic data, the code reads many different exchanger configurations from the tube count table and calculates the pressure drop, required heat transfer area and exchanger length for each configuration and then selects the one that has the smallest exchanger area for lowering the initial cost. Finally, in other references (Gloyer, 1950; Girish *et al.*, 2017; Elakkiyadasan *et al.*, 2021) the design and sizing of shell and tube condensers is carried out. Also, some textbooks present several worked examples of the design of condensers, such as (Smith, 2005; Kakaç *et al.*, 2012; Cao, 2010; Thulukkanam, 2013; Nitsche & Gbadamosi, 2016) and (Sinnott & Towler, 2020), using heuristics based on choices made by the designer.

In a Cuban chemical processing plant, it is desired to condense a vapour stream of pure ethanol coming from the top of a rectification column, and for that a horizontal shell and tube heat exchanger is considered. Accordingly, in the present work the thermo-hydraulic design of a shell and tube heat exchanger is carried out in order to condense this vapour stream of pure ethanol. Several design parameters are determined for the heat exchanger such as the heat exchanged, heat transfer area, number of tubes, overall heat transfer coefficient and the pressure drop of both streams. To accomplish this task, the design methodology reported by (Sinnott & Towler, 2020) is used.

2. MATERIALS AND METHODS

2.1. Problem definition

It is desired to condense 25,000 kg/h of a vapour stream of ethanol using chilled water at an inlet temperature of 5 °C. The vapour will enter the condenser saturated at 90 °C and 4 bar, and the condensation will be complete at 52 °C. The outlet temperature of the chilled water must not exceed 15 °C. Plant standards require tubes of 20 mm outside diameter, 16.8 mm inside diameter, 4.88 m (16 ft.) long, of stainless steel 316. The vapours are to be totally condensed and no sub-cooling is required. A pressure drop of 12,000 and 45,000 Pa is permissible for the ethanol and water streams, respectively. Design a horizontal shell and tube condenser operating under counter-current flow and having one shell pass and two tube passes. Use the design methodology reported in (Sinnott & Towler, 2020) for this heat transfer task.

2.2. Required initial data

- Molecular weight of ethanol (M_{et}).
- Inlet temperature of ethanol (T_1).
- Condensation temperature of ethanol (T_c).
- Inlet pressure of vapour ethanol (P).
- Inlet temperature of chilled water (t_1).
- Outlet temperature of chilled water (t_2).
- Mass flowrate of vapour ethanol (m_{et}).
- Enthalpy of ethanol at vapour state [$h_{et(v)}$].
- Enthalpy of ethanol at liquid (condensate) state [$h_{et(L)}$].
- Inside diameter of tube (d_i).
- Outside diameter of tube (d_o).
- Tube length (L_t).
- Number of tube-side passes (n_t).
- Gravitational acceleration (g).
- Fouling factor of ethanol (R_{et}).
- Fouling factor of water (R_w).
- Thermal conductivity of stainless steel (k_{ss}).

2.3. Design parameters of the condenser

Step 1. Heat transferred from vapour (Q):

$$Q = \frac{m_{et}}{3600} \cdot [h_{et(v)} - h_{et(L)}] \quad (1)$$

Step 2. Assumption of the overall heat transfer coefficient (U_o):

A value of the overall heat transfer coefficient (U_0) must be initially assumed, taking into account the values suggested by (Sinnott & Towler, 2020) for this kind of heat transfer service.

Step 3. Parameter R:

$$R = \frac{(T_1 - T_c)}{(t_2 - t_1)} \quad (2)$$

Step 4. Parameter S:

$$S = \frac{(t_2 - t_1)}{(T_1 - t_1)} \quad (3)$$

Step 5. Allocation of the fluids inside the heat exchanger.

Step 6. Log mean temperature difference (ΔT_{lm}) for counter-current flow:

$$\Delta T_{lm} = \frac{(T_1 - t_2) - (T_c - t_1)}{\ln \frac{(T_1 - t_2)}{(T_c - t_1)}} \quad (4)$$

Step 7. Temperature correction factor (F_t):

For a 1 shell, 2 tube pass exchanger, the correction factor is given by the following correlation (Sinnott & Towler, 2020).

$$F_t = \frac{\sqrt{(R^2 + 1)} \cdot \ln \left[\frac{(1 - S)}{(1 - R \cdot S)} \right]}{(R - 1) \cdot \ln \left[\frac{2 - S \cdot \left[R + 1 - \sqrt{(R^2 + 1)} \right]}{2 - S \cdot \left[R + 1 + \sqrt{(R^2 + 1)} \right]} \right]} \quad (5)$$

Step 8. True temperature difference (ΔT_m):

$$\Delta T_m = \Delta T_{lm} \cdot F_t \quad (6)$$

Step 9. Trial area (A_0):

$$A_0 = \frac{Q}{U_0 \cdot \Delta T_m} \cdot 1000 \quad (7)$$

Where Q is given in kW.

Step 10. Surface area of one tube (a_t):

$$a_t = \pi \cdot d_o \cdot L_t \quad (8)$$

Where d_o is given in m.

Step 11. Number of tubes (N_{t0}):

$$N_{t0} = \frac{A_0}{a_t} \quad (9)$$

Step 12. Selection of tube pitch (distance between tube centres):

The tubes in a heat exchanger are usually arranged in an equilateral triangular, square, or rotated square pattern. The triangular and rotated square patterns give higher heat-transfer rates, but at the expense of a higher pressure drop than the square pattern. A square, or rotated square arrangement, is used for heavily fouling fluids, where it is necessary to mechanically clean the outside of the tubes. The recommended tube pitch (distance between tube centers) is 1.25 times the tube outside diameter (Sinnott & Towler, 2020).

Step 13. Tube pitch (p_t):

$$p_t = 1.25 \cdot d_o \quad (10)$$

Where d_o is given in mm.

Step 14. Tube bundle diameter (D_b):

The bundle diameter depends not only on the number of tubes but also on the number of tube passes, as spaces must be left in the pattern of tubes on the tube sheet to accommodate the pass partition plates.

$$D_b = d_o \cdot \left(\frac{N_{t0}}{K_1} \right)^{1/n_1} \quad (11)$$

Where d_o is given in mm, while K_1 and n_1 are constants that depend on the number of tube passes and the pitch selected, which values can be found in (Sinnott & Towler, 2020).

Step 15. Number of tubes in center row (N_r):

$$N_r = \frac{D_b}{p_t} \quad (12)$$

Where both D_b and p_t are given in mm.

Step 16. Assumption of the mean condensation film coefficient ($h_{c(a)}$):

Step 17. Mean temperature of both the shell-side and tube-side fluids:

In case that the condensing vapour (hot fluid) is allocated in the shell side of the heat exchanger, the mean temperature of this fluid is determined by the following equation:

$$\bar{T} = \frac{T_1 + T_c}{2} \quad (13)$$

While the mean temperature of the tube-side fluid (cold fluid) is calculated by the following equation:

$$\bar{t} = \frac{t_1 + t_2}{2} \quad (14)$$

Step 18. Tube wall temperature (T_w):

$$(\bar{T} - T_w) \cdot h_{c(a)} = (\bar{T} - \bar{t}) \cdot U_0 \quad (15)$$

Step 19. Mean temperature of condensate (\bar{T}_c):

$$\bar{T}_c = \frac{\bar{T} + T_w}{2} \quad (16)$$

Step 20. Physical properties of the condensate at the mean temperature \bar{T}_c :

- Density (ρ_L).
- Viscosity (μ_L).
- Thermal conductivity (k_L).

Step 21. Vapour ethanol density (ρ_v) at the mean vapour temperature (\bar{T}):

$$\rho_v = \frac{M_{et}}{22.4} \cdot \frac{273}{(273 + \bar{T})} \cdot \frac{P}{P_0} \quad (17)$$

Where $P_0 = 1$ bar.

Step 22. Condensate loading on a horizontal tube (Γ_h):

$$\Gamma_h = \frac{m_{et}}{3600} \cdot \frac{1}{L_t \cdot N_{r0}} \quad (18)$$

Step 23. Average number of tubes in a vertical tube row (N_{tr}):

$$N_{tr} = \frac{2}{3} \cdot N_r \quad (19)$$

Step 24. Mean condensation film coefficient for a tube bundle ($h_{c(c)}$):

$$h_{c(c)} = 0.95 \cdot k_L \cdot \left[\frac{\rho_L \cdot (\rho_L - \rho_v) \cdot g}{\mu_L \cdot \Gamma_h} \right]^{1/3} \cdot N_{tr}^{-1/6} \quad (20)$$

Step 25. Verification of the calculated mean condensation film coefficient of step 20 ($h_{c(c)}$) with respect to the assumed condensation film coefficient in step 14 ($h_{c(a)}$).

Step 26. Tube cross sectional area (a_{ct}):

$$a_{ct} = \frac{\pi}{4} \cdot d_i^2 \cdot \frac{N_{t10}}{n_t} \quad (21)$$

Where d_i is given in meters.

Step 27. Density of the tube side fluid at \bar{t} (ρ_t).

Step 28. Heat capacity of the cold fluid (cooling water) at \bar{t} (Cp_c).

Step 29. Required flow of the cold fluid (cooling water) (m_c):

$$m_c = \frac{Q}{(t_2 - t_1) \cdot Cp_c} \quad (22)$$

Step 30. Velocity of the tube side fluid (u_t):

$$u_t = \frac{m_c}{\rho_t \cdot a_{ct}} \quad (23)$$

Step 31. Tube side heat transfer coefficient (h_t):

For water (Sinnott & Towler, 2020):

$$h_t = \frac{4,200 \cdot (1.35 + 0.02 \cdot \bar{t}) \cdot u_t^{0.8}}{d_i^{0.2}} \quad (24)$$

Where d_i is given in mm.

Step 32. Calculated overall heat transfer coefficient (U):

$$U = \frac{1}{\frac{1}{h_{c(c)}} + R_{et} + \frac{d_o \cdot \ln\left(\frac{d_o}{d_i}\right)}{2 \cdot k_{ss}} + \frac{d_o}{d_i} \cdot R_w + \frac{d_o}{d_i} \cdot \frac{1}{h_t}} \quad (25)$$

Where both d_o and d_i are given in meters.

The overall heat transfer coefficient calculated in step 32 must be compared with the assumed value of step 2.

2.4. Pressure drop

The pressure drop on the condensing side is difficult to predict as two phases are present and the vapour mass velocity is changing throughout the condenser. A common practice is to calculate the pressure drop using the methods for single-phase flow and apply a factor to allow for the change in vapour velocity. For total condensation, (Frank, 1978) suggests taking the pressure drop as 40 % of the value based on the inlet vapour conditions, while (Kern, 1950) suggests a factor of 50 %.

Shell side:

Step 33. Clearance required between the outermost tubes in the bundle (C_t):

As reported by (Sinnott & Towler, 2020), the clearance will depend on the type of heat exchanger and the bundle diameter (D_b), and typical values are given in this reference for four types of heat exchangers, which are the following:

- Pull-through floating head.
- Split-ring floating head.
- Outside packed head.
- Fixed and U-tube.

Step 34. Shell internal diameter (D_s):

$$D_s = D_b + C_t \quad (26)$$

Where both D_b and C_t are given in meters.

Step 35. Select baffle spacing (l_B) and baffle cut:

The baffle spacings used range from 0.2 to 1.0 shell diameters. A close baffle spacing will give higher heat-transfer coefficients, but at the expense of higher pressure drop. The optimum spacing will usually be between 0.3 to 0.5 times the shell diameter. On the other hand, the term “baffle cut” is used to specify the dimensions of a segmental baffle, and it is the height of the segment removed to form the baffle, expressed as a percentage of the baffle disc diameter. Baffle cuts from 15 to 45 % are used. Generally, a baffle cut of 20 to 25% will be the optimum, giving good heat-transfer rates without excessive pressure drop (Sinnott & Towler, 2020).

Step 36. Cross-flow area between tubes (A_s):

$$A_s = \frac{(p_t - d_o) \cdot D_s \cdot l_B}{p_t} \quad (27)$$

Where all the parameters are given in meters.

Step 37. Shell-side mass velocity (G_s):

$$G_s = \frac{m_{et}}{3600} \cdot \frac{1}{A_s} \quad (28)$$

Step 38. Shell-side linear velocity (u_s):

$$u_s = \frac{G_s}{\rho_v} \quad (29)$$

Step 39. Shell-side equivalent diameter (hydraulic diameter) (d_e):

- For square pitch arrangement:

$$d_e = \frac{1.27}{d_o} \cdot (p_t^2 - 0.785 \cdot d_o^2) \quad (30)$$

- For an equilateral triangular pitch arrangement:

$$d_e = \frac{1.10}{d_o} \cdot (p_t^2 - 0.917 \cdot d_o^2) \quad (31)$$

Where all the parameters are given in meters.

Step 40. Vapour viscosity of the condensing fluid (μ_v) at the mean temperature (\bar{T}).

Step 41. Vapour Reynolds number (Re_v):

$$Re_v = \frac{G_s \cdot d_e}{\mu_v} \quad (32)$$

Step 42. Shell-side friction factor (j_s):

The shell-side friction factor (j_s) is determined depending on the values obtained for the Reynolds number and the baffle cut, as indicated by (Sinnott & Towler, 2020).

Step 43. Shell side pressure drop (ΔP_s):

The shell side pressure drop can be taken as 50 % of that calculated using the inlet flow; while the viscosity correction factor can be neglected (Sinnott & Towler, 2020). Thus:

$$\Delta P_s = \frac{1}{2} \cdot \left[8 \cdot j_s \cdot \left(\frac{D_s}{d_e} \right) \cdot \left(\frac{L_t}{l_B} \right) \cdot \frac{\rho_v \cdot u_s^2}{2} \right] \quad (33)$$

Where D_s , d_e , L_t and l_B are given in meters.

Tube side:

Step 44. Viscosity of the tube side fluid at \bar{t} (μ_t).

Step 45. Reynolds number of the tube side fluid (Re_t):

$$Re_t = \frac{u_t \cdot \rho_t \cdot d_i}{\mu_t} \quad (34)$$

Step 46. Tube-side friction factor (j_t).

The tube-side friction factor depends on the Reynolds number of the tube-side fluid, as reported by (Sinnott & Towler, 2020).

Step 47. Tube-side pressure drop (ΔP_t):

$$\Delta P_t = n_t \cdot \left[8 \cdot j_t \cdot \left(\frac{L_t}{d_i} \right) \cdot \left(\frac{\mu_t}{\mu_w} \right)^{-m} + 2.5 \right] \cdot \frac{\rho_t \cdot u_t^2}{2} \quad (35)$$

As suggested by (Sinnott & Towler, 2020), the viscosity correction factor $(\mu_t / \mu_w)^{-m}$ can be neglected.

3. RESULTS AND DISCUSSION

3.1. Initial data required

The Table 1 shows the initial data required to design the horizontal shell and tube condenser.

Table 1. Initial data required to design the horizontal shell and tube condenser.

Parameter	Symbol	Value	Units
Molecular weight of ethanol ¹	M_{et}	46.07	kg/kmol
Inlet temperature of ethanol	T_1	90	°C
Condensation temperature of ethanol	T_c	52	°C
Inlet pressure of vapour ethanol	P	4	bar
Inlet temperature of chilled water	t_1	5	°C
Outlet temperature of chilled water	t_2	15	°C
Mass flowrate of vapour ethanol	m_{et}	25,000	kg/h
Enthalpy of ethanol at vapour state ¹	$h_{et(v)}$	1281.37	kJ/kg
Enthalpy of ethanol at liquid (condensate) state ¹	$h_{et(L)}$	334.01	kJ/kg
Inside diameter of tube	d_i	0.0168	m

Outside diameter of tube	d_o	0.02	m
Tube length	L_t	4.88	m
Number of tube-side passes	n_t	2	-
Gravitational acceleration	g	9.81	m/s ²
Fouling factor of ethanol ²	R_{et}	0.00020	m ² .°C/W
Fouling factor of water ²	R_c	0.00025	m ² .°C/W
Thermal conductivity of stainless steel ³	k_{ss}	16	W/m.°C

¹ As reported by (Vine & Wormald, 1989).

² As reported by (Sinnott & Towler, 2020).

³ As reported by (Peters et al., 2003).

Source: Own elaboration.

3.2. Design parameters of the condenser

The Table 2 presents the results of the parameters calculated in steps 1-4.

Table 2. Results of the parameters calculated in steps 1-4.

Step	Parameter	Symbol	Value	Units
1	Heat transferred from vapour	Q	6,578.47	kW
2	Assumption of the overall heat transfer coefficient	U_o	500	W/m ² .°C
3	Parameter	R	3.80	-
4	Parameter	S	0.12	-

Source: Own elaboration.

Step 5. Allocation of the fluids inside the heat exchanger:

Taking into account the suggestions stated by (Sinnott & Towler, 2020), the ethanol stream will be allocated on the shell-side, while the water will flow on the tube-side.

The Table 3 shows the results of the parameters determined in steps 6-24.

Table 3. Results of the parameters determined in steps 6-24.

Step	Parameter	Symbol	Value	Units
6	Log mean temperature difference	ΔT_{lm}	59.96	°C
7	Temperature correction factor	F_t	0.981	-
8	True temperature difference	ΔT_m	58.82	°C
9	Trial area	A_0	223.68	m ²
10	Surface area of one tube	a_t	0.306	m ²
11	Number of tubes	N_{t0}	731	-
12	Selection of tube pitch	-	Triangular	-
13	Tube pitch	p_t	25	mm
14	Tube bundle diameter ¹	D_b	744.57	mm
15	Number of tubes in centre row	N_r	30	-

16	Assumption of the mean condensation film coefficient	$h_{c(a)}$	800	W/m ² .°C
17	Mean temperature of both fluids	\bar{T}	71	°C
		\bar{t}	10	°C
18	Tube wall temperature	T_w	32.88	°C
19	Mean temperature of condensate	\bar{T}_c	51.94	°C
	Density of ethanol condensate ²	ρ_L	311.14	kg/m ³
20	Viscosity of ethanol condensate ²	μ_L	0.00066	Pa.s
	Thermal conductivity of ethanol condensate ²	k_L	0.1610	W/m.K
21	Vapour ethanol density	ρ_v	6.53	kg/m ³
22	Condensate loading on a horizontal tube	Γ_h	0.0019	kg/m.s
23	Average number of tubes in a vertical tube row	N_{tr}	20	-
24	Mean condensation film coefficient for a tube bundle	$h_{c(c)}$	829.38	W/m ² .°C

¹The values of the constants K_1 and n_1 used to determine this parameter are 0.249 and 2.207, respectively (Sinnott & Towler, 2020).

²As reported by (Green & Southard, 2019).

Source: Own elaboration.

Step 25. Verification of the calculated mean condensation film coefficient of step 20 ($h_{c(c)}$) with respect to the assumed condensation film coefficient in step 14 ($h_{c(a)}$).

Since the calculated value of $h_{c(c)}$ (829.38 W/m².°C) is close enough to that assumed in step 24 for $h_{c(a)}$ (800 W/m².°C), there is no need for further iteration. In this case, the value of $h_{c(c)}$ will be used to calculate the overall heat transfer coefficient (U).

The Table 4 describes the results of the parameters calculated in steps 26-32

Table 4. Results of the parameters calculated in steps 26-32

Step	Parameter	Symbol	Value	Units
26	Tube cross sectional area	a_{ct}	0.081	m ²
27	Density of the tube side fluid (water) ¹	ρ_t	999.70	kg/m ³
28	Heat capacity of the cooling water ¹	Cp_c	4.205	kJ/kg.K
29	Required flow of cooling water	m_c	156.44	kg/s
30	Velocity of the tube side fluid	u_t	1.93	m/s
31	Tube side heat transfer coefficient	h_t	6,265.59	W/m ² .°C
32	Calculated overall heat transfer coefficient	U	499.36	W/m ² .°C

¹As reported by (Green & Southard, 2019).

Source: Own elaboration.

3.3. Shell side pressure drop

Step 33. Clearance required between the outermost tubes in the bundle (C_t):

The type of heat exchanger selected in this work was the pull-through floating head, while the required value of the clearance is 0.94 m for a value of the bundle diameter of 744.57 mm, as indicated by (Sinnott & Towler, 2020).

Step 34. Shell internal diameter (D_s):

$$D_s = D_b + C_t = 0.744 + 0.94 = 1.684 \text{ m} \quad (26)$$

Step 35. Baffle spacing (l_B) and baffle cut:

According to the suggestions of (Sinnott & Towler, 2020), the baffle spacing will be 0.4 times the shell internal diameter, thus:

$$l_B = 0.4 \cdot D_s = 0.674 \text{ m}$$

In the case of the baffle cut, the value selected was 25%.

The Table 5 exposes the results of the parameters determined in steps 36-43.

Table 5. Results of the parameters determined in steps 36-43.

Step	Parameter	Symbol	Value	Units
36	Cross-flow area between tubes	A_s	0.227	m
37	Shell-side mass velocity	G_s	30.59	kg/s.m ²
38	Shell-side linear velocity	u_s	4.68	m/s
39	Shell-side equivalent diameter (for triangular pitch arrangement)	d_e	0.0142	m
40	Vapour viscosity of ethanol	μ_v	0.0000102	Pa.s
41	Vapour Reynolds number	Re_v	42,586.08	-
42	Shell-side friction factor ¹	j_s	0.041	-
43	Shell side pressure drop	ΔP_s	10,069.25	Pa

¹ For a value of 42,586.08 for the Reynolds number and a baffle cut of 25%.
Source: Own elaboration.

3.4. Tube side pressure drop

The Table 6 shows the results of the parameters calculated in steps 44-47.

Table 6. Results of the parameters calculated in steps 44-47.

Step	Parameter	Symbol	Value	Units
44	Viscosity of water	μ_t	0.00130	Pa.s
45	Reynolds number of the tube side fluid	Re_t	24,934.06	-
46	Tube-side friction factor	j_t	0.0038	-

Source: Own elaboration.

The value of the calculated overall heat transfer coefficient was 499.36 W/m².°C, which is almost equal to the value assumed for this parameter in step 2 (500 W/m².°C), therefore no further iteration is required. Considering this, the designed shell and tube heat exchanger should present the following preliminary design parameters:

- Exchanger type: Pull-through floating head.
- Tube bundle diameter: 744.57 mm.
- Number of tubes: 731.
- Heat transfer area: 223.68 m².
- Clearance: 0.94 m.
- Shell internal diameter: 1.684 m.
- Baffle spacing: 0.674 m.
- Baffle cut: 25%.

The value of the tube side heat transfer coefficient ($h_t = 6,265.59$ W/m².°C) was 7.55 times higher than the value of the calculated mean condensation film coefficient for ethanol ($h_{c(e)} = 829.38$ W/m².°C). In (Sinnott & Towler, 2020), the value of h_t is 4.90 times higher than the value of $h_{c(e)}$ for a shell and tube heat exchanger designed to condense 45,000 kg/h of mixed light hydrocarbons using cooling water available at 30 °C. In (Sahajpal & Shah, 2013) the tube side heat transfer coefficient has a value of 6,567.32 W/m².°C, while the shell side heat transfer coefficient is 11,836.27 W/m².°C adding up the two heat transfer coefficients corresponding to the desuperheating and condensation regions. It can be observed that in (Sahajpal & Shah, 2013) the opposite occurs as compared to the results obtained in this study and in those reported by (Sinnott & Towler, 2020), that is, the shell side heat transfer coefficient is 1.80 times higher than the tube side heat transfer coefficient. It's worth stating that in (Sahajpal & Shah, 2013) a shell and tube condenser was also designed using HTRI software, and the results obtained from this software were 7,081.82 and 4,995.21 W/m².°C for the tube side and shell side heat transfer coefficients, respectively. That is, the tube side heat transfer coefficient is 1.42 times higher than the shell side coefficients, which corresponds and agrees with the results obtained of this study and those stated by (Sinnott & Towler, 2020).

The required mass flowrate of chilled water was 156.44 kg/s, which could be considered relatively high, while the value of the heat transferred was 6,578.47 kW. In (Sinnott & Towler, 2020), the flowrate of cooling water necessary to condense 12.5 kg/s of a stream of mixed light hydrocarbons is 104.5 kg/s, while the heat transferred is 4,368.8 kW. In (Sahajpal & Shah, 2013), the flowrate of cooling water required to condense 0.6841 kg/s of ammonia is 35.97 kg/s, whereas the heat transferred reported in this study is 903.78 kW.

The heat transfer area calculated in this study was 223.68 m², while in (Sinnott & Towler, 2020) the value of the heat transfer area is 364 m² and in (Sahajpal & Shah, 2013) the value of this parameters is 116.62 m².

The shell internal diameter determined in this study was 1.684 m, while in (Sinnott & Towler, 2020) the value of this parameter is 1.130 m for a pull-through floating head heat exchanger, and in (Sahajpal & Shah, 2013) the value of D_s is 0.840 m for a TEMA AES shell and tube heat exchanger.

The shell side pressure drop had a value of 10,069.25 Pa, while the tube side pressure drop was 42,192.63 Pa, that is, both values are below the maximum values established by the process, which are 12,000 and 45,000 Pa for ethanol and water respectively. In this case, the tube side pressure drop was 4.19 times higher than the shell side pressure drop. In (Sinnott & Towler, 2020), the value of the shell side pressure drop is 1,322 Pa, while the value of the tube side pressure drop is 53,388 Pa, that is, the tube side pressure drop is 40.38 times higher than the shell side pressure drop. In (Sahajpal & Shah, 2013), the shell side pressure drop is 1,223.4 Pa and the tube side pressure drop is 49,130 Pa, i.e. the tube side pressure drop is 40.16 times higher than the shell side pressure drop. The higher value obtained in this study for the shell side pressure drop, as compared to the values obtained in (Sinnott & Towler, 2020) and (Sahajpal & Shah, 2013), could be due to the high values obtained for both the shell-side linear velocity (4.68 m/s) and the shell internal diameter (1.684 m). It's worth mentioning that in (Sinnott & Towler, 2020) the value of both the shell-side linear velocity and the shell internal diameter are 2.51 m/s and 1,130 m, respectively, while in the case of (Sahajpal & Shah, 2013), the values of both parameters are 1.78 m/s and 0.840 m, respectively. That is, in both studies the values reported for those parameters are below the values obtained in this work, thus influencing in the lower values obtained for the shell side pressure drop.

4. CONCLUSIONS

A horizontal shell and tube heat exchanger was designed in order to condense 25,000 kg/h of a pure ethanol stream, using chilled water available at 5 °C. Several design parameters were calculated; such as the tube bundle diameter (744.57 mm), number of tubes (731), heat transfer area (223.68 m²), shell internal diameter (1.684 m), baffle spacing (0.674 m) and baffle cut (25%). The heat transferred from vapour had a value of 6,578.47 kW, while the overall heat transfer coefficient was 499.36 W/m².°C. About 157 kg/s of chilled water are required to carry out the condensation service, and both the shell-side (10,069.25 Pa) and the tube-side pressure drops (42,192.63 Pa) are below the maximum values established by the process. The designed shell and tube heat exchanger will be of pull-through floating head type.

REFERENCES

- Bell, K. J. (1963). Final Report of the Cooperative Research Program on Shell-And-Tube Heat Exchangers. University of Delaware Engineering Experiment Station Bulletin No. 5. Newark, USA: University of Delaware.
- Cao, E. (2010). Heat transfer in process engineering. New York, USA: McGraw-Hill.
- Chen, L.-Y., Adi, V. S. K., & Laxmidewi, R. (2022). Shell and tube heat exchanger flexible design strategy for process operability. *Case Studies in Thermal Engineering*, 37, 102163. <https://doi.org/10.1016/j.csite.2022.102163>
- Deng, S. (2000). A dynamic mathematical model of a direct expansion (DX) water-cooled air-conditioning plant. *Building and Environment*, 35, 603–613.
- Elakkiyadasan, R., Kumar, P. M., Subramanian, M., Balaji, N., Karthick, M., & Kaliappan, S. (2021). Optimization of Shell and Tube Condenser for Low Temperature Thermal Desalination Plant. *E3S Web of Conferences*, 309, 01011. <https://doi.org/10.1051/e3sconf/202130901011>
- Feng, H., Cai, C., Chen, L., Wu, Z., & Lorenzini, G. (2020). Constructural design of a shell-and-tube condenser with ammonia-water working fluid. *International Communications in Heat and Mass Transfer*, 118, 104867. <https://doi.org/10.1016/j.icheatmasstransfer.2020.104867>
- Flynn, A. M., Akashige, T., & Theodore, L. (2019). *Kern's Process Heat Transfer*. Hoboken, USA: John Wiley & Sons, Inc.
- Frank, O. (1978). Simplified design procedure for tubular exchangers. *Practical Aspects of Heat Transfer*. Chemical Engineering Progress Technical Manual: American Institute of Chemical Engineers.

- Girish, S., Prakash, M. S., Krishna, P. G., & Lavanya, K. (2017). Analysis of a condenser in a thermal power plant for possible augmentation in its heat transfer performance. *International Journal of Civil Engineering and Technology*, 8 (7), 410–420.
- Gloyer, W. (1950). *Thermal Design of Condensers*. *Industrial and Engineering Chemistry*, 42 (7), 1361-1369.
- Green, D. W., & Southard, M. Z. (2019). *Perry's Chemical Engineers' Handbook* (9th ed.). New York, USA: McGraw-Hill Education.
- Hajabdollahi, H., Ahmadi, P., & Dincer, I. (2011). Thermoeconomic optimization of a shell and tube condenser using both genetic algorithm and particle swarm. *International Journal of Refrigeration*, 34, 1066-1076. <https://doi.org/10.1016/j.ijrefrig.2011.02.014>
- Kakaç, S., Liu, H., & Pramuanjaroenkij, A. (2012). *Heat Exchangersa. Selection, Rating, and Thermal Design*. Boca Raton, USA: CRC Press.
- Kapooria, R. K., Kumar, S., & Kasana, K. S. (2008). Technological investigations and efficiency analysis of a steam heat exchange condenser: conceptual design of a hybrid steam condenser. *Journal of Energy in Southern Africa*, 19 (3), 35-45.
- Kara, Y. A. (2014). A simplified three-zone model for designing shell-and-tube refrigerant condensers. *Journal of Thermal Science and Technology*, 34 (1), 9-18.
- Karlsson, T., & Vamling, L. (2005). Flow fields in shell-and-tube condensers: comparison of a pure refrigerant and a binary mixture. *International Journal of Refrigeration*, 28, 706–713. <https://doi.org/10.1016/j.ijrefrig.2004.12.008>
- Kern, D. Q. (1950). *Process Heat Transfer*. New York, USA: McGraw-Hill.
- Lim, T.-W., & Choi, Y.-S. (2020). Thermal design and performance evaluation of a shell-and-tube heat exchanger using LNG cold energy in LNG fuelled ship. *Applied Thermal Engineering*, 171, 115120. <https://doi.org/10.1016/j.applthermaleng.2020.115120>
- Llopis, R., Cabello, R., & Torrella, E. (2008). A dynamic model of a shell-and-tube condenser operating in a vapour compression refrigeration plant. *International Journal of Thermal Sciences*, 47, 926–934. <https://doi.org/10.1016/j.ijthermalsci.2007.06.021>
- Milián, V., Navarro-Esbrí, J., Ginestar, D., Molés, F., & Peris, B. (2013). Dynamic model of a shell-and-tube condenser. Analysis of the mean void fraction correlation influence on the model performance. *Energy*, 59, 521-533. <http://dx.doi.org/10.1016/j.energy.2013.07.053>
- Nithyanandam, K., Shoaie, P., & Pitchumani, R. (2021). Technoeconomic analysis of thermoelectric power plant condensers with nonwetting surfaces. *Energy*, 227, 120450. <https://doi.org/10.1016/j.energy.2021.120450>
- Nitsche, M., & Gbadamosi, R. O. (2016). *Heat Exchanger Design Guide*. Oxford, UK: Butterworth Heinemann.
- Pereira, I. P. S., Bagajewicz, M. J., & Costa, A. L. H. (2021). Global optimization of the design of horizontal shell and tube condensers. *Chemical Engineering Science*, 236, 116474. doi:<https://doi.org/10.1016/j.ces.2021.116474>
- Peters, M. S., Timmerhaus, K. D., & West, R. E. (2003). *Plant Design and Economics for Chemical Engineers* (5th ed.). New York, USA: McGraw-Hill.
- Sahajpal, S., & Shah, P. D. (2013). Thermal Design of Ammonia Desuperheater-Condenser and Comparative Study with HTRI. *Procedia Engineering*, 51, 375 – 379. <https://doi.org/10.1016/j.proeng.2013.01.052>
- Sinnott, R., & Towler, G. (2020). *Chemical Engineering Design* (6th ed.). Oxford, United Kingdom: Butterworth-Heinemann.
- Smith, E. M. (2005). *Advances in Thermal Design of Heat Exchangers*. Hoboken, USA: John Wiley & Sons Inc.

Soltan, B. K., Saffar-Avval, M., & Damangir, E. (2004). Minimizing capital and operating costs of shell and tube condensers using optimum baffle spacing. *Applied Thermal Engineering*, 24, 2801–2810. <https://doi.org/10.1016/j.applthermaleng.2004.04.005>

Thulukkanam, K. (2013). *Heat Exchanger Design Handbook* (2nd ed.). Boca Raton, USA: CRC Press.

Vine, M. D., & Wormald, J. (1989). The enthalpy of ethanol. *J. Chem. Thermodynamics*, 21, 1151-1157.

SEMBLANCE OF THE AUTHORS



Amaury Pérez Sánchez: Obtained a degree in Chemical Engineering from the University of Camagüey, Cuba, in 2009, where he is currently an Instructor Professor and assistant researcher. At the moment he is studying a Master in Biotechnology at the Center for Genetic Engineering and Biotechnology in Camagüey. He works in research lines related fundamentally with the design of heat and mass transfer equipment, simulation and optimization of processes and operations in the chemical industry using simulators such as SuperPro Designer® and ChemCAD®, and the techno-economic evaluation of processes and biotechnological plants.



Maria Isabel La Rosa Veliz: Obtained the degree of Chemical Engineering from the University of Camagüey, Cuba, in the year 2023. She currently works as a professor and researcher at the University of Camagüey. Her lines of research are related to biotechnology, specifically with the scale up of broad-spectrum vaccines against ticks, as well as the simulation and optimization of biotechnological processes through the use of SuperPro Designer® and MATLAB®. She is studying a Master's Degree in Analysis of Chemical Processes at the University of Camagüey.



Zamira María Sarduy Rodríguez: Obtained the degree of Chemical Engineering from the University of Camagüey, Cuba, in the year 2023. She currently works as a professor and researcher at the University of Camagüey. Her research lines involve the industrial scale up of broad-spectrum vaccines against ticks, as well as the simulation and optimization of processes using software such as SuperPro Designer® and MATLAB®. She is studying a Master's Degree in Analysis of Chemical Processes at the University of Camagüey.



Elizabeth Ranero González: Obtained a degree of Chemical Engineering from the University of Camagüey, Cuba, in 2016. She works professionally as Instructor Professor at the University of Camagüey, Cuba. Her research area includes the design and rating of heat and mass transfer equipment and processes, thermodynamic evaluation of chemical processes, and the simulation of biotechnological processes and systems.



Eddy Javier Pérez Sánchez: Obtained a degree in Chemical Engineering from the University of Camagüey, Cuba, in 2016. He works professionally at Empresa de Servicios Automotores S.A., in the Department of Commercial Management. His research lines include the design, rating and/or operation of heat and mass transfer equipment, as well as the simulation of petrochemical and biotechnological processes.